







Operation of a High Renewable Penetrated Power System With CSP Plants: A Look-Ahead Stochastic Unit Commitment Model

Ershun Du , Member, IEEE, Ning Zhang , Senior Member, IEEE, Bri-Mathias Hodge, Senior Member, IEEE, Qin Wang , Member, IEEE, Zongxiang Lu , Member, IEEE, Chongqing Kang , Fellow, IEEE, Benjamin Kroposki, Fellow, IEEE, and Qing Xia , Senior Member, IEEE

Abstract—The integration of variable renewable energy (VRE) generation, i.e., wind power and solar photovoltaic, brings significant uncertainty for the power system operation. Different with VRE techniques, concentrating solar power (CSP) is an appealing renewable generation technology due to its dispatch ability through the use of thermal energy storage and is thus expected to play a significant role in high renewable energy penetrated power systems. In this paper, we propose a look-ahead stochastic unit commitment model to operate power systems with CSP under high renewable energy penetration. It has a three-stage structure. The first stage optimizes the operational decisions in a day-ahead framework based on forecasts; the second stage minimizes the expected generation cost for possible realizations in the real time; and the third stage accounts for look-ahead operation in future operating days. This paper has a dual purpose: first, exploring how CSP plants operate in high renewable penetrated power systems; and second, analyzing the benefits of CSP in accommodating VRE generation. A case study on a modified IEEE RTS-79 system with actual solar and wind power data is provided to validate the proposed method.

Index Terms—Concentrating solar power, energy storage, high share of renewable energy, operational flexibility, stochastic unit commitment.

NOMENCLATURE

A. Subscripts

b	Index of storage device from 1 to N_B .
c	Index of CSP plant from 1 to N_{CSP} .
g	Index of conventional unit from 1 to N_G .

Manuscript received October 25, 2017; revised March 7, 2018 and June 27, 2018; accepted August 12, 2018. Date of publication August 28, 2018; date of current version December 19, 2018. This work was supported in part by the National Key R&D Program of China under Grant 2016YFB0900100, in part by the National Natural Science Foundation of China under Grant 51677096, and in part by the Scientific and Technical Project of State Grid. Paper no. TPWRS-01613-2017. (Corresponding authors: Ning Zhang and Zongxiang Lu.)

E. Du, N. Zhang, Z. Lu, C. Kang, and Q. Xia are with the State Key Laboratory of Power Systems, Electrical Engineering Department, Tsinghua University, Beijing 10084, China (e-mail: des13@mails.tsinghua.edu.cn; ningzhang@tsinghua.edu.cn; luzongxiang98@mail.tsinghua.edu.cn; cqkang@tsinghua.edu.cn; qingxia@tsinghua.edu.cn).

B.-M. Hodge, Q. Wang, and B. Kroposki are with the National Renewable Energy Laboratory, Golden, CO 80401 USA (e-mail: Bri.Mathias.Hodge@nrel.gov; qwang@epri.com; benjamin.kroposki@nrel.gov).

Color versions of one or more of the figures in this paper are available online at <http://ieeexplore.ieee.org>.

Digital Object Identifier 10.1109/TPWRS.2018.2866486

k	Index of time period from 1 to N_K for the third-stage model.
l	Index of transmission line from 1 to N_L .
m	Index of third-stage scenario from 1 to N_M .
n	Index of node bus from 1 to N_N .
s	Index of second-stage scenario from 1 to N_S .
t	Index of time period from 1 to N_T .
v	Index of photovoltaic station from 1 to N_{PV} .
w	Index of wind farm from 1 to N_W .

B. Superscripts

G, B, PV, W, CSP	Representing conventional thermal units, battery storage devices, photovoltaic stations, wind farms and CSP units, respectively.
TES, PB, SF, EH	Denoting thermal energy storage, power block, solar field and electric heater in CSP plants, respectively.

C. Parameters

C	Generating cost of a power plant [\$/MW-e].
D	Forecasting load [MW-e].
DF	Branch power flow distribution factor.
$E^{PB, SU}$	Start-up power of CSP plants [MWh-t].
$\bar{E}^{TES}, \underline{E}^{TES}$	Max/min state-of-charge of TES [MWh-t].
F^{Max}	Line capacity [MW-e].
H^B	Energy storage time [h].
P^{Max}, P^{Min}	Max/min generation limits [MW-e].
P^{Fore}	Forecasting generation of PV/Wind [MW-e].
$R^{Ru, Sys}, R^{Rd, Sys}$	System up/down reserve requirement [MW-e].
SF^{Fore}	Forecasting solar thermal power [MW-t].
SU	Starting up cost of a power plant [\$].
$T_{min}^{On}, T_{min}^{Off}$	Minimum on/off times of a power plant [h].
$\Delta P^{Rus}, \Delta P^{Rd}$	Up/down ramping rate [MW-e/h].
Δt	Time interval of dispatching.

θ^{VoLL}	Penalty cost of load shedding [\$/MWh].
π	Occurrence probability.
η^{cha}, η^{dis}	Charging/discharging efficiency.
η^{PB}, η^{EH}	PB/EH efficiency.
γ^{TES}	Heat dissipation factor of TES.
$\Omega^{CSP}(\ast)$	Feasible operation space of a CSP plant.

D. Variables

Variables with tilde (\sim) denote the ones in the second-stage model, those with hat ($\hat{\cdot}$) denote the ones in the third-stage model, and the rest without accents are the ones in the first-stage model.

E^{TES}/E^B	State-of-charge (SOC) of TES [MWh-t]/SOC of battery storage devices [MWh-e].
f	Power flow of transmission line [MW-e].
I^{cha}/I^{dis}	Charging/discharging binary variables.
P	Electricity Power output [MW-e].
P^{Cur}/L^{Cur}	Renewable energy/load curtailment [MW-e].
R/r	Scheduled/deployed reserves [MW-e].
x, u	Unit status/start-up binary variables.

I. INTRODUCTION

A. Background

GLOBAL warming and fossil fuel depleting are pushing electric energy power systems to be transformed from being thermal generator dominated into renewable dominated systems [1]. Some countries like Denmark and Ireland are already operating a power grid with more than 20% annual electricity generation from wind power and solar photovoltaics (PV). However, renewable energy production highly depends on the weather condition and thus is associated with large variability and uncertainty [2]. This brings great challenges for the power system operation and necessitates considerable operational flexibility.

In this light, concentrating solar power (CSP) is an appealing renewable generation technology due to its dispatch-ability through the use of thermal energy storage (TES) and is thus expected to play a significant role in high renewable energy penetrated power systems [3]. Specifically, CSP transforms solar irradiation into heat that can be stored in TES during the daytime and generates electricity as needed. Even if little solar irradiation is available on some cloudy days, a large enough TES system allows CSP to shift electric production between different days. Besides, TES also allows CSP to cooperate with electric heaters (EH) to convert electricity from the grid into thermal energy that is re-used at a later time. Generally, CSP equipped with TES and EH provides an alternative choice to supply operational flexibility in power systems to help the balance between load and generation in an uncertainty environment. These attributes will help to facilitate the integration of variable renewable energy (VRE) such as wind power and PV in high renewable penetrated power systems.

In this paper, we focus on the short-term operation of a high renewable penetrated power system with CSP plants and analyze the role of CSP in accommodating VRE generation.

B. Literature Review

Operation of high renewable energy penetrated power systems is attracting increasing attentions [4]–[7]. The National Renewable Energy Laboratory (NREL) in U.S. has presented a report *Renewable Electricity Future Study* [8] to analyze the scenario where a large part of electricity load demand is supplied by renewable energy sources for the U.S. power system in 2050. This study concludes that it is feasible to achieve a renewable-dominated power system with 80% generation capacity from renewable sources in 2050, and CSP is expected to be a significant part in the generation portfolio. Another NREL report [9] specifically analyzed the value of CSP in integrating large scale renewable energy generation through a case study on the U.S. southwestern electric system. Dominguez *et al.* [10] explored whether it is possible to achieve a fully renewable power system. The results show that CSP will play a significant role to ensure the power balance.

Currently, many researches are concerning about the strategic operation of CSP plants and analyzing the cost-benefits of CSP [11]–[13]. Majority of them consider the strategic operation of CSP to maximize its profit in an electricity market as a price-taker [14], [15] or in co-operation with VRE [16], [17]. Fewer studies analyze the CSP behaviors from the prospective of power system operation. Chen *et al.* [18] reformulated the power system scheduling model to take CSP into consideration and analyzed the benefits of CSP in reducing system operating costs and VRE curtailment, but the uncertainties of VRE and CSP were not considered. Jin *et al.* [19] proposed a multi-day stochastic operation model for power systems with CSP to make full use of TES. Xu and Zhang [20] utilized a stochastic unit commitment (SUC) and a look-ahead economic dispatch (ED) with considering wind/CSP uncertainty to simulate the operation of a power system with CSP and quantify the value of CSP for the provision of energy and reserve services. Denholm *et al.* [21] compared the economic value among CSP, base-load units and PV, based on a whole year production simulation for the California power system with 33% renewable portfolio standard. Dominguez *et al.* [22] simulated the CSP operation in a fully renewable power system and illustrated the significant role of CSP to hedge the variability and uncertainty of VRE generation.

One of key challenges of operating a high penetrated power system is how to strategically schedule flexible generating sources under large scale uncertain renewable energy generation supply. Zheng *et al.* [23] summarized the SUC approaches to operate power systems under uncertainty and illustrated the benefits of stochastic optimization. Morales *et al.* [24] proposed a stochastic scheduling approach with co-optimizing energy and reserves, and evaluated the economic value of operating reserves in power systems with high wind power penetration. Bakirtzis *et al.* [25] proposed a multiple time resolution unit commitment (UC) model to optimize the short-term generation schedule under high renewable energy penetration. Denholm and Hand [26] analyzed the role of storage in renewable dominated power systems. Pozo *et al.* [27] addressed how to incorporate a generic energy storage model into the SUC model, considering the use

of energy storage for shifting generation and providing reserves. The look-ahead scheduling model is widely used to manage the state-of-charge (SOC) of the storage [28], [29].

C. Contributions

In this paper, we propose an improved stochastic scheduling model to strategically operate a power system with CSP plants under high renewable energy penetrations. The proposed model simultaneously optimizes energy and reserve scheduling decisions, considering the uncertainties of wind speed and solar irradiation which are modeled by multiple scenarios. The CSP plant equipped with TES and EH is modeled in detail and operates strategically to provide both dispatchable generation and operating reserves to facilitate the integration of VRE.

Compared with a co-located VRE and storage design, CSP essentially can be regarded as a storage with a variable and uncertain charging source. TES can be built large enough to allow CSP to shift generation between different days to hedge the intermittency of solar irradiation. Hence, the day-ahead operation schedule of CSP should not only consider the operation situation of the next operating day, but also take into account how much energy should be stored in the TES at the end of next operating day for the operation at future days.

In order to address the above issue, a look-ahead SUC model is proposed. It has a three-stage structure. The first stage optimizes the scheduling decisions including both energy and reserves at the day-ahead time scale. The second stage employs a real-time re-dispatch process to eliminate the power imbalance between day-ahead schedules and RT actuals for each realizable scenario. The third-stage accounts for look-ahead operation in future operating days to optimize the SOC of TES in each scenario at the end of next operating day. Compared with existing multi-stage stochastic programming methods to optimize the operation of energy storage devices, such as [30] and [31], the proposed model is more of an extension of a two-stage SUC model considering look-ahead operation.

Taking into account the above background and literature review, the contributions of this paper are three-fold:

- 1) Proposing a generic operation model of CSP with TES and EH towards the short-term power system operation scheduling.
- 2) Incorporating the CSP operation model into a look-ahead stochastic unit commitment model that makes full use of the flexibility of CSP in high renewable penetrated systems.
- 3) Analyzing the benefits of CSP in facilitating the integration of VRE generation.

The rest of the paper is organized as follows. Section II describes the operation model of CSP with TES and EH. Section III formulates the proposed look-ahead stochastic unit commitment model. A case study on a modified IEEE RTS-79 system is provided in Section IV to verify the effectiveness of proposed model. Section V concludes the paper.

II. CSP MODEL WITH TES AND EH

Fig. 1 provides a general configuration for CSP plants, including four encapsulated blocks, namely solar field (SF), TES

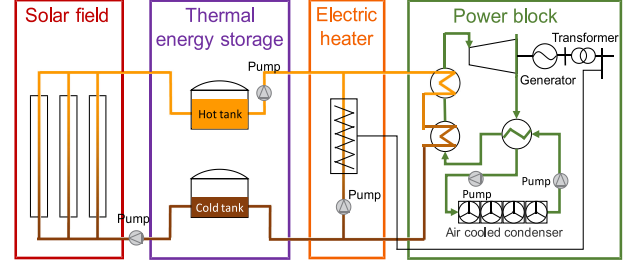


Fig. 1. Configuration of a CSP plant.

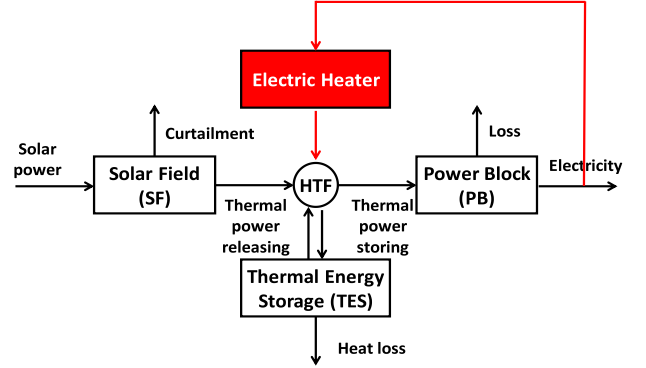


Fig. 2. Simplified energy flow in CSP with TES and EH.

system, power block (PB) and electric heater (EH). Heat transfer fluid (HTF) flows through these blocks to deliver thermal energy. The SF concentrates solar irradiation and heats the HTF. Then high-temperature HTF can flow into the power block to generate high-temperature steam that is used to drive a steam turbine to produce electricity. HTF can also flow into the TES system to store or release thermal energy. EH can be equipped with CSP to expand the feasible range of CSP outputs and allows for CSP to convert electricity from the grid into thermal energy for use at a later time. Fig. 2 illustrates the schematic energy flow framework in a CSP plant equipped with TES and EH systems.

Many references have presented various CSP operation models. Detailed CSP operation model for the self-operation/control study can be found in [32]. Simplified steady-state dispatch model of CSP is proposed in [15] and [22]. Based on these results, a more generic and comprehensive dispatch model of CSP is proposed and can be easily incorporated into power system scheduling problems. A configuration of CSP equipped with TES and EH is considered.

Through analyzing the thermal energy balance in each encapsulated block in CSP, a mixed-integer linear constraint set is proposed to describe the feasible operating space of CSP.

$$\begin{aligned}
 \Omega_c^{CSP}(\{SF_{c,t}^{Fore}, \forall t\}) &= \left\{ P_{c,t}^{CSP}, P_{c,t}^{EH}, P_{c,t}^{TES,cha}, P_{c,t}^{TES,dis}, E_{c,t}^{TES}, x_{c,t}^{CSP}, \forall t \right\} \\
 &\times \left(SF_{c,t}^{Fore} - P_{c,t}^{CSP,Cur} / \eta_c^{PB} \right) + \eta_c^{EH} P_{c,t}^{EH} \\
 &= \left(P_{c,t}^{TES,cha} / \eta_c^{TES,cha} - P_{c,t}^{TES,dis} / \eta_c^{TES,dis} \right) + P_{c,t}^{PB,in}, \forall t
 \end{aligned} \quad (1)$$

$$P_{c,t}^{PB,in} \approx f(P_{c,t}^{CSP}) = P_{c,t}^{CSP} / \eta_c^{PB} + u_{c,t}^{PB} E_c^{PB,SU}, \forall t \quad (2)$$

$$E_{c,t}^{TES} = (1 - \gamma_c^{TES}) E_{c,t-1}^{TES} + (P_{c,t}^{TES,cha} - P_{c,t}^{TES,dis}) \Delta t, \forall t > 1 \quad (3)$$

$$\underline{E}_{c,t}^{TES} \leq E_{c,t}^{TES} \leq \bar{E}_{c,t}^{TES}, \forall t \quad (4)$$

$$0 \leq P_{c,t}^{TES,dis} \leq I_{c,t}^{TES,dis} P_c^{TES,Max}, \forall t \quad (5)$$

$$0 \leq P_{c,t}^{TES,cha} \leq I_{c,t}^{TES,cha} P_c^{TES,Max}, \forall t \quad (6)$$

$$I_{c,t}^{TES,cha} + I_{c,t}^{TES,dis} \leq 1; x_{c,t}^{PB} \geq I_{c,t}^{TES,dis}, \forall t \quad (7)$$

$$x_{c,t}^{PB} P_c^{PB,Min} \leq P_{c,t}^{CSP} \leq x_{c,t}^{PB} P_c^{PB,Max}, \forall t \quad (8)$$

$$(x_{c,t}^{PB} - x_{c,t-1}^{PB}) T_{c,min}^{On,CSP} + \sum_{\tau=t-T_{c,min}^{On,CSP}-1}^{t-1} x_{c,\tau}^{PB} \geq 0, \forall t > 1 \quad (9)$$

$$(x_{c,t-1}^{PB} - x_{c,t}^{PB}) T_{c,min}^{Off,CSP} + \sum_{\tau=t-T_{c,min}^{Off,CSP}-1}^{t-1} (1 - x_{c,\tau}^{PB}) \geq 0, \forall t > 1 \quad (10)$$

$$x_{c,t}^{PB} - x_{c,t-1}^{PB} \leq u_{c,t}^{PB}, u_{c,t}^{PB} \leq x_{c,t}^{PB}, u_{c,t}^{PB} \leq 1 - x_{c,t-1}^{PB}, \forall t > 1 \quad (11)$$

$$P_{c,t}^{CSP} - P_{c,t-1}^{CSP} + x_{c,t-1}^{PB} (P_c^{PB,Min} - \Delta P_c^{Ru,PB}) + x_{c,t}^{PB} (P_c^{PB,Max} - P_c^{PB,Min}) \leq P_c^{PB,Max}, \forall t > 1 \quad (12)$$

$$P_{c,t-1}^{CSP} - P_{c,t}^{CSP} + x_{c,t}^{PB} (P_c^{PB,Min} - \Delta P_c^{Rd,PB}) + x_{c,t-1}^{PB} (P_c^{PB,Max} - P_c^{PB,Min}) \leq P_c^{PB,Max}, \forall t > 1 \quad (13)$$

$$0 \leq P_{c,t}^{EH} \leq P_c^{PB,Max}, \forall t \quad (14)$$

$$P_{c,t}^{Net} = P_{c,t}^{CSP} - P_{c,t}^{EH}, \forall t \quad (15)$$

Constraint (1) represents the instantaneous thermal power balance in CSP plants. The total thermal energy input is equal to the sum of thermal energy absorbed from the SF ($SF_{c,t}^{Fore}$) and the thermal energy transferred from EH ($\eta_c^{EH} P_{c,t}^{EH}$). The possible spill is modeled by variable $P_{c,t}^{CSP,Cur}$. The thermal energy is consumed via the energy exchange in TES and the consumption by PB ($P_{c,t}^{PB,in}$). Constraint (2) denotes the function between the thermal energy input in PB ($P_{c,t}^{PB,in}$) and the electricity output of PB ($P_{c,t}^{CSP}$) [15]. This function can be approximated by piece-wise linear functions. For simplicity, a constant generating efficiency η_c^{PB} is assumed, and $E_c^{PB,SU}$ denotes the start-up energy needed to begin generating electricity [22]. Constraint (3) models the thermal energy balance in the TES system. The heat dissipation of TES is modeled by introducing a dissipation factor γ_c^{TES} [18]. Constraint (4) depicts the feasible operation interval of the SOC of TES. Constraints (5) and (6) set the charging and discharging rates within the operation bound $[0, P_c^{TES,Max}]$ if only if the corresponding state variable is 1. Constraint (7) guarantees that the charging and discharging states will not occur simultaneously and that the discharging state will occur only when the PB is on.

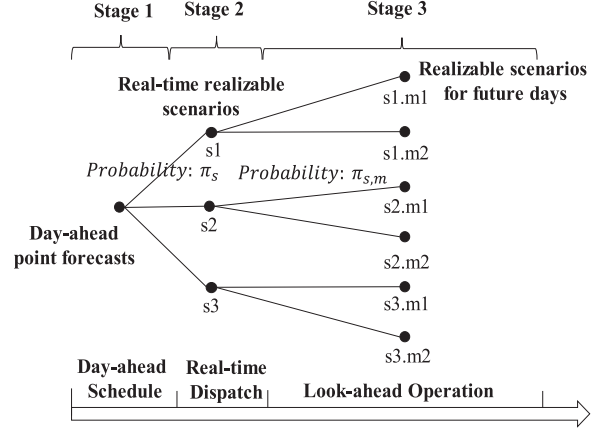


Fig. 3. Uncertainty representation: A three-stage scenario tree.

The PB module has similar operational constraints as a conventional unit [33]. Specifically, constraints (8) and (9) formulate the minimum on/off time limit. Constraint (10) describes the relationship between the on/off state variables and the starting-up variable. Constraint (11) sets the generation output within the operation bound $[P_c^{PB,Min}, P_c^{PB,Max}]$ if only if the PB is on-line. Constraints (12) and (13), respectively, formulate the up/down ramping rate limits. Constraint (14) assumes that the electricity consumption of EH is not more than the electricity generation capacity of CSP. Constraint (15) formulates the net output of CSP with TES and EH, $P_{c,t}^{Net}$, which locates in the interval $[-P_c^{PB,Max}, P_c^{PB,Max}]$.

The produced thermal energy in the SF, $SF_{c,t}^{Fore}$, is modeled as the input parameter. If given the value of solar irradiation, software tool SAM (Solar Advisor Model, developed by NREL) [34] can be used to convert solar irradiation into produced solar thermal power in SF ($SF_{c,t}^{Fore}$) for CSP plants.

III. UNIT-COMMITMENT MODEL FORMULATION

A. Model Framework

A look-ahead SUC model is proposed to optimize the generation schedule of high renewable penetrated power systems with CSP plants. The proposed model simultaneously optimizes energy and reserve scheduling decisions, considering the uncertainties of wind speed and solar irradiation. These uncertain inputs are modeled by a three-stage scenario tree shown in Fig. 3. The proposed model has a three-stage structure. The first stage optimizes the UC decisions in a day-ahead framework based on point forecasting results, the second stage eliminates the imbalance power for all possible realizations in the real-time based on economic dispatch (ED) operation, and the third stage accounts for the look-ahead ED operation in future operating days to optimize the SOC of TES in each scenario at the end of next operating day. The SUC model is optimized to minimize the overall expected operating cost. Only the decisions for the coming operating day are put into practice. The decisions for future operating days are for look-ahead operation evaluation.

The variables associated with each stage are explained as follows. For the first stage, variables include 1) the start-up and

shut-down decisions of each unit, 2) scheduled power output of each unit, 3) scheduled down/up spinning reserve of each unit and 4) power flow on each branch. These variables are called *here and now* decisions and do not depend on any particular scenario realization. For the second stage, the variables pertain to each particular scenario for real-time re-dispatch, including: 1) the deployment of down/up spinning reserve of each unit, 2) the renewable energy curtailment, 3) the load shedding at each node bus, 4) actual power flow on each branch. These variables are called *wait and see* decisions. For the third stage, the variables also pertain to each particular scenario but are related to the look-ahead operation in future days, including: 1) generation schedule of each unit, 2) power flow on each branch. These variables are called *look-ahead* decisions.

B. Model Formulation

1) Objective Function:

$$\text{minimize } Cost^{Sys} = Cost^{DA} + Cost^{RT} + Cost^{LA}$$

where:

$$\begin{aligned} Cost^{DA} &= \sum_{t=1}^{N_T} \sum_{g=1}^{N_G} \left(SU_g^G u_{g,t}^G + C_g^G P_{g,t}^G + C_g^{Ru} R_{g,t}^{Ru} + C_g^{Rd} R_{g,t}^{Rd} \right) \\ Cost^{RT} &= \sum_{s=1}^{N_S} \pi_s \left\{ \sum_{t=1}^{N_T} \left\{ \sum_{g=1}^{N_G} \tilde{C}_g^G \left(\tilde{R}_{g,t,s}^{Ru} - \tilde{R}_{g,t,s}^{Rd} \right) \right. \right. \\ &\quad \left. \left. + \sum_{c=1}^{N_{CSP}} C_c^{CSP} \tilde{P}_{c,t,s}^{CSP} + \theta^{VoLL} \sum_{n=1}^{N_N} \tilde{L}_{n,t,s}^{Cur} \right\} \right\} \\ Cost^{LA} &= \sum_{s=1}^{N_S} \pi_s \left\{ \sum_{m=1}^{N_M} \pi_{s,m} \left\{ \sum_{k=1}^{N_K} \left\{ \sum_{g=1}^{N_G} C_g^G \hat{P}_{g,k,s,m}^G \right. \right. \right. \\ &\quad \left. \left. + \sum_{c=1}^{N_{CSP}} C_c^{CSP} \hat{P}_{c,k,s,m}^{CSP} + \theta^{VoLL} \sum_{n=1}^{N_N} \hat{L}_{n,k,s,m}^{Cur} \right\} \right\} \right\} \end{aligned} \quad (16)$$

The objective function (16) minimizes the overall expected operating cost, $Cost^{Sys}$. The first part is the day-ahead generation scheduling cost $Cost^{DA}$, including the start-up cost, fuel cost, and up/down spinning reserve scheduling cost for all conventional units. The second part is the expected real-time dispatch cost $Cost^{RT}$, including reserve deployment cost of conventional units, the generating cost of CSP plants, and the penalty cost of involuntary load shedding. The third part is the expected look-ahead operating cost $Cost^{LA}$ in future days.

2) *First-Stage Constraints*: First-stage constraints are formulated with day-ahead point forecasts of wind power and solar power. Constraint (17) ensures the system load-generation balance at each time slot.

$$\begin{aligned} \sum_{g=1}^{N_G} P_{g,t}^G + \sum_{w=1}^{N_W} P_{w,t}^W + \sum_{v=1}^{N_{PV}} P_{v,t}^{PV} + \sum_{b=1}^{N_B} \left(P_{b,t}^{B,dis} - P_{b,t}^{B,cha} \right) \\ + \sum_{c=1}^{N_{CSP}} \left(P_{c,t}^{CSP} - P_{c,t}^{EH} \right) \\ = \sum_{n=1}^{N_N} \left(D_{n,t} - L_{n,t}^{Cur} \right), L_{n,t}^{Cur} \in [0, D_{n,t}], \forall t \end{aligned} \quad (17)$$

For each conventional thermal unit, constraints (18) and (19) represent the ramping up/down rate limit. The minimum on/off time limit for each unit is considered by constraints (20) and (21). Constraint (22) describes the relationship between the unit status and the starting-up action. Constraint (23) ensures that the online conventional unit is scheduled to offer both energy $P_{g,t}^G$ and up (down) reserve $R_{g,t}^{Ru}$ ($R_{g,t}^{Rd}$) without violating its operating bound $[P_{g,t}^{G,Min}, P_{g,t}^{G,Max}]$.

$$P_{g,t}^G - P_{g,t-1}^G + x_{g,t-1}^G (P_{g,t}^{G,Min} - \Delta P_{g,t}^{G,Ru}) + x_{g,t}^G (P_{g,t}^{G,Max} - P_{g,t}^{G,Min}) \leq P_{g,t}^{G,Max}, \forall t > 1, \forall g \quad (18)$$

$$P_{g,t-1}^G - P_{g,t}^G + x_{g,t}^G (P_{g,t}^{G,Min} - \Delta P_{g,t}^{G,Rd}) + x_{g,t-1}^G (P_{g,t}^{G,Max} - P_{g,t}^{G,Min}) \leq P_{g,t}^{G,Max}, \forall t > 1, \forall g \quad (19)$$

$$\left(x_{g,t}^G - x_{g,t-1}^G \right) T_{g,min}^{On,G} + \sum_{\tau=t-T_{g,min}^{On,G}-1}^{t-1} x_{g,\tau}^G \geq 0, \forall t > 1, \forall g \quad (20)$$

$$\left(x_{g,t-1}^G - x_{g,t}^G \right) T_{g,min}^{Off,G} + \sum_{\tau=t-T_{g,min}^{Off,G}-1}^{t-1} \left(1 - x_{g,\tau}^G \right) \geq 0, \forall t > 1, \forall g \quad (21)$$

$$x_{g,t}^G - x_{g,t-1}^G \leq u_{g,t}^G, u_{g,t}^G \leq x_{g,t}^G, u_{g,t}^G \leq 1 - x_{g,t-1}^G, \forall t > 1, \forall g \quad (22)$$

$$P_{g,t}^G - R_{g,t}^{Rd} \geq x_{g,t}^G P_{g,t}^{G,Min}; P_{g,t}^G + R_{g,t}^{Ru} \leq x_{g,t}^G P_{g,t}^{G,Max}; R_{g,t}^{Ru}, R_{g,t}^{Rd} \geq 0, \forall t, \forall g \quad (23)$$

As for renewable generating units, constraints (24) and (25) limit the schedule of a wind or PV plant not more than its forecasting output value.

$$P_{w,t}^W + P_{w,t}^{W,Cur} = P_{w,t}^{W,Fore}; P_{w,t}^W, P_{w,t}^{W,Cur} \geq 0, \forall t, \forall w \quad (24)$$

$$P_{v,t}^{PV} + P_{v,t}^{PV,Cur} = P_{v,t}^{PV,Fore}; P_{v,t}^{PV}, P_{v,t}^{PV,Cur} \geq 0, \forall t, \forall v \quad (25)$$

For energy storage systems (ESS), constraint (26) limits the charging and discharging rates within the operation bound $[0, P_{b,t}^{B,Max}]$. Constraints (27) and (28) formulate the energy balance in ESS. Constraint (29) limits the SOC level not more than the energy storage capacity ($H_b^B P_{b,t}^{B,Max}$). The ESS is able to provide operating reserves. Constraints (30) and (31), respectively, schedule the up/down reserves provided by ESS with not violating the charging/discharging power capacity.

$$0 \leq P_{b,t}^{B,dis} \leq \left(1 - I_{b,t}^{B,cha} \right) P_{b,t}^{B,Max}, 0 \leq P_{b,t}^{B,cha} \leq I_{b,t}^{B,cha} P_{b,t}^{B,Max}, \forall t, \forall b \quad (26)$$

$$E_{b,t}^B - E_{b,t-1}^B = \left(P_{b,t}^{B,cha} / \eta_b^{B,cha} - P_{b,t}^{B,dis} \eta_b^{B,dis} \right) \Delta t, \forall t > 1, \forall b \quad (27)$$

$$E_{b,t}^B - E_b^{B,ini} = \left(P_{b,t}^{B,cha} / \eta_b^{B,cha} - P_{b,t}^{B,dis} \eta_b^{B,dis} \right) \Delta t, \forall t = 1, \forall b \quad (28)$$

$$0 \leq E_{b,t}^B \leq H_b^B P_b^{B,Max}, \forall t, \forall b \quad (29)$$

$$P_{b,t}^{B,cha} - P_{b,t}^{B,dis} + R_{b,t}^{B,Ru} \leq P_b^{B,Max}; R_{b,t}^{B,Ru} \geq 0, \forall t, \forall b \quad (30)$$

$$P_{b,t}^{B,dis} - P_{b,t}^{B,cha} + R_{b,t}^{B,Rd} \leq P_b^{B,Max}; R_{b,t}^{B,Rd} \geq 0, \forall t, \forall b \quad (31)$$

For each CSP plant, the operating position should be located in the feasible operation space $\Omega_c^{CSP}(\{SF_{c,t}^{Fore}, \forall t\})$, formulated by constraint (32). Constraints (33) to (36) formulate the up/down spinning reserve scheduling constraints. Specifically, shown in constraint (33), when the PB is on-line, the up reserve provided by the PB is not more than the room $(P_{c,t}^{PB,Max} - P_{c,t}^{CSP})$ and the room of available TES discharging. Constraint (34) sets the up reserve provided by EH not more than the generation schedule of EH. Similarly, down reserves provided by the PB and EH can be formulated by constraints (35) and (36).

$$(P_{c,t}^{CSP}, P_{c,t}^{EH}) \in \Omega_c^{CSP}(\{SF_{c,t}^{Fore}, \forall t\}), \forall t, \forall c \quad (32)$$

$$0 \leq R_{c,t}^{PB,Ru} \leq x_{c,t}^{PB} * \min(P_{c,t}^{PB,Max} - P_{c,t}^{CSP}, (E_{c,t}^{TES} - E_{c,t}^{TES})\eta_c^{PB}), \forall t, \forall c \quad (33)$$

$$0 \leq R_{c,t}^{EH,Ru} \leq P_{c,t}^{EH}, \forall t, \forall c \quad (34)$$

$$0 \leq R_{c,t}^{PB,Rd} \leq x_{c,t}^{PB} * \min(P_{c,t}^{CSP} - P_{c,t}^{PB,Min}, (E_{c,t}^{TES} - E_{c,t}^{TES})\eta_c^{PB}), \forall t, \forall c \quad (35)$$

$$0 \leq R_{c,t}^{EH,Rd} \leq P_{c,t}^{PB,Max} - P_{c,t}^{EH}, \forall t, \forall c \quad (36)$$

Constraint (37) formulates the branch power flow limit. Constraints (38) and (39) form the minimum system up and down reserve requirements.

$$f_{l,t} = \sum_{g=1}^{N_G} DF_{l,g} P_{g,t}^G + \sum_{w=1}^{N_W} DF_{l,w} P_{w,t}^W + \sum_{v=1}^{N_{PV}} DF_{l,v} P_{v,t}^{PV} + \sum_{b=1}^{N_B} DF_{l,b} (P_{b,t}^{B,dis} - P_{b,t}^{B,cha}) + \sum_{c=1}^{N_{CSP}} DF_{l,c} (P_{c,t}^{CSP} - P_{c,t}^{EH}) - \sum_{n=1}^{N_N} DF_{l,n} (D_{n,t} - L_{n,t}^{Cur}) \in [-F_l^{Max}, F_l^{Max}], \forall t, \forall l \quad (37)$$

$$\sum_{g=1}^{N_G} R_{g,t}^{G,Ru} + \sum_{b=1}^{N_B} R_{b,t}^{B,Ru} + \sum_{c=1}^{N_{CSP}} (R_{c,t}^{PB,Ru} + R_{c,t}^{EH,Ru}) \geq R^{Ru,Sys}, \forall t \quad (38)$$

$$\sum_{g=1}^{N_G} R_{g,t}^{G,Rd} + \sum_{b=1}^{N_B} R_{b,t}^{B,Rd} + \sum_{c=1}^{N_{CSP}} (R_{c,t}^{PB,Rd} + R_{c,t}^{EH,Rd}) \geq R^{Rd,Sys}, \forall t \quad (39)$$

3) *Second-Stage Constraints:* To represent the wind and solar power uncertainty, N_S scenarios representing real-time possible realizations of renewable energy production are considered

in second-stage constraints. These constraints describe how the scheduled reserves in the first stage are deployed to eliminate the power imbalance between day-ahead schedules and real-time actuals.

Specifically, constraint (40) represents the load-generation balance in each scenario. The branch power flow constraint in (41) is the same as constraint (37) but modified for the second stage variables.

$$\begin{aligned} & \sum_{g=1}^{N_G} \tilde{P}_{g,t,s}^G + \sum_{w=1}^{N_W} \tilde{P}_{w,t,s}^W + \sum_{v=1}^{N_{PV}} \tilde{P}_{v,t,s}^{PV} + \sum_{b=1}^{N_B} (\tilde{P}_{b,t,s}^{B,dis} - \tilde{P}_{b,t,s}^{B,cha}) \\ & + \sum_{c=1}^{N_{CSP}} (\tilde{P}_{c,t,s}^{CSP} - \tilde{P}_{c,t,s}^{EH}) \\ & = \sum_{n=1}^{N_N} (D_{n,t} - \tilde{L}_{n,t,s}^{Cur}), \tilde{L}_{n,t,s}^{Cur} \in [0, D_{n,t}], \forall t, \forall s \end{aligned} \quad (40)$$

Modified version of (37) (41)

For each conventional unit, the operating constraints are the same as those in the first-stage. The dispatched power output is equal to its day-ahead scheduled output plus the real-time deployed reserves.

Modified versions of (18) and (19) (42)

$$x_{g,t}^G P_{g,t}^{G,Min} \leq \tilde{P}_{g,t,s}^G \leq x_{g,t}^G P_{g,t}^{G,Max}, \forall t, \forall g, \forall s \quad (43)$$

$$\tilde{P}_{g,t,s}^G = P_{g,t}^G + \tilde{r}_{g,t,s}^{G,Ru} - \tilde{r}_{g,t,s}^{G,Rd}, \forall t, \forall g, \forall s \quad (44)$$

$$0 \leq \tilde{r}_{g,t,s}^{G,Ru} \leq R_{g,t}^{G,Ru}, 0 \leq \tilde{r}_{g,t,s}^{G,Rd} \leq R_{g,t}^{G,Rd}, \forall t, \forall g, \forall s \quad (45)$$

For each wind and PV plant:

Modified versions of (24)–(25) (46)

For each EES, the operating constraints are the same as those in the first-stage. Constraints (48) and (49) link the scheduled ESS operation and actual ESS operation.

Modified versions of (26)–(28) (47)

$$\begin{aligned} \tilde{p}_{b,t,s}^{B,dis} - \tilde{p}_{b,t,s}^{B,cha} &= P_{b,t}^{B,dis} - P_{b,t}^{B,cha} + \tilde{r}_{b,t,s}^{B,Ru} \\ &\quad - \tilde{r}_{b,t,s}^{B,Rd}, \forall t, \forall b, \forall s \end{aligned} \quad (48)$$

$$0 \leq \tilde{r}_{b,t,s}^{B,Ru} \leq R_{b,t}^{B,Ru}, 0 \leq \tilde{r}_{b,t,s}^{B,Rd} \leq R_{b,t}^{B,Rd}, \forall t, \forall b, \forall s \quad (49)$$

For each CSP unit, the PB status is fixed. The real-time dispatch position should be located in the feasible operation space. The dispatched power output is equal to the day-ahead scheduled output plus the real-time deployed reserves. Deployed reserves from the power block and EH are limited not exceeding the scheduled values in the first stage.

$$(\tilde{P}_{c,t,s}^{CSP}, \tilde{P}_{c,t,s}^{EH}) \in \Omega_c^{CSP}(\{SF_{c,t,s}^{Fore}, \forall t\}), \forall t, \forall c, \forall s \quad (50)$$

$$\tilde{x}_{c,t,s}^{CSP} = x_{c,t}^{CSP}, \forall t, \forall c, \forall s \quad (51)$$

$$\tilde{P}_{c,t,s}^{CSP} = P_{c,t}^{CSP} + \tilde{r}_{c,t,s}^{PB,Ru} - \tilde{r}_{c,t,s}^{PB,Rd}, \forall t, \forall c, \forall s \quad (52)$$

$$0 \leq \tilde{r}_{c,t,s}^{PB,Ru} \leq R_{c,t}^{PB,Ru}, 0 \leq \tilde{r}_{c,t,s}^{PB,Rd} \leq R_{c,t}^{PB,Rd}, \forall t, \forall c, \forall s \quad (53)$$

$$\tilde{P}_{c,t,s}^{EH} = P_{c,t}^{EH} + \tilde{r}_{c,t,s}^{EH,Ru} - \tilde{r}_{c,t,s}^{EH,Rd}, \forall t, \forall c, \forall s \quad (54)$$

$$0 \leq \tilde{r}_{c,t,s}^{EH,Ru} \leq R_{c,t}^{EH,Ru}, 0 \leq \tilde{r}_{c,t,s}^{EH,Rd} \leq R_{c,t}^{EH,Rd}, \forall t, \forall c, \forall s \quad (55)$$

4) *Third-Stage Constraints*: The third-stage model simulates the look-ahead operation for future days, and the generation schedule is not put into practice. Thus, a simplified linear operation model is employed and binary UC decisions are not considered, in order to improve the computation performance. Specifically, ED operational constraints are incorporated in the third-stage to optimize the residual SOC of TES and ESS at the end of the next operating day for each scenario.

Constraint (56) represents the system load-generation balance. Constraint (57) includes the branch power flow limit and the operating constraints for VRE units.

$$\begin{aligned} & \sum_{g=1}^{N_G} \hat{P}_{g,k,s,m}^G + \sum_{w=1}^{N_W} \hat{P}_{w,k,s,m}^W + \sum_{v=1}^{N_{PV}} \hat{P}_{v,k,s,m}^{PV} \\ & + \sum_{b=1}^{N_B} \left(\hat{P}_{b,k,s,m}^{B,dis} - \hat{P}_{b,k,s,m}^{B,cha} \right) + \sum_{c=1}^{N_{CSP}} \left(\hat{P}_{c,k,s,m}^{CSP} - \hat{P}_{c,k,s,m}^{EH} \right) \\ & = \sum_{n=1}^{N_N} \left(D_{n,k,s,m} - \hat{L}_{n,k,s,m}^{Cur} \right), \hat{L}_{n,k,s,m}^{Cur} \in [0, D_{n,k,s,m}], \\ & \quad \forall k, \forall s, \forall m \end{aligned} \quad (56)$$

$$\text{Modified versions of (24), (25) and (37)} \quad (57)$$

For conventional thermal units, the on/off state variables are neglected, and the feasible generation output is from 0 to its power capacity, shown in constraint (58). Constraints (59) and (60) formulate the up/down ramping rate limit.

$$0 \leq \hat{P}_{g,k,s,m}^G \leq P_g^{G,Max}, \forall k, \forall g, \forall s, \forall m \quad (58)$$

$$\begin{aligned} -\Delta P_g^{G,Rd} & \leq \hat{P}_{g,k,s,m}^G - \hat{P}_{g,k-1,s,m}^G \\ & \leq \Delta P_g^{G,Rd}, \forall k > 1, \forall g, \forall s, \forall m \end{aligned} \quad (59)$$

$$\begin{aligned} -\Delta P_g^{G,Rd} & \leq \hat{P}_{g,k,s,m}^G - \tilde{P}_{g,t=T,s}^G \\ & \leq \Delta P_g^{G,Rd}, \forall k = 1, \forall g, \forall s, \forall m \end{aligned} \quad (60)$$

Constraints (61)–(68) formulate a simplified operational model for CSP plants. Specifically, constraints (61)–(64) simulate the operation of the power block and EH. Constraints (65) formulates the thermal energy balance in TES. The discharging rate of TES is related to the electricity generation of CSP $\hat{P}_{c,k,s,m}^{CSP}$, while the charging rate of TES includes the absorbed solar thermal energy from SF and the transferred thermal energy from EH. Constraint (66) links the SOC of TES in the second-stage with that in the third stage. The SOC of TES is limited within $[\bar{E}_c^{TES}, \bar{E}_c^{TES}]$ via constraint (67). Constraint (68) ensures the SOC of TES to go back to its initial value $E_c^{TES,Ini}$ at

the end of the simulating time horizon.

$$\begin{aligned} -\Delta P_c^{Rd} & \leq \hat{P}_{c,k,s,m}^{CSP} - \hat{P}_{c,k-1,s,m}^{CSP} \leq \Delta P_c^{Rd}, \forall k > 1, \forall c, \forall s, \forall m \\ -\Delta P_c^{Rd} & \leq \hat{P}_{c,k,s,m}^{CSP} - \tilde{P}_{c,t=N_T,s}^{CSP} \leq \Delta P_c^{Rd}, \forall k = 1, \forall c, \forall s, \forall m \end{aligned} \quad (61)$$

$$0 \leq \hat{P}_{c,k,s,m}^{CSP} \leq P_c^{PB,Max}, \forall k, \forall c, \forall s, \forall m \quad (63)$$

$$0 \leq \hat{P}_{c,k,s,m}^{EH} \leq P_c^{PB,Max}, \forall k, \forall c, \forall s, \forall m \quad (64)$$

$$\begin{aligned} \hat{E}_{c,k,s,m}^{TES} & = \hat{E}_{c,k-1,s,m}^{TES} - \left(\hat{P}_{c,k,s,m}^{CSP} / \eta_c^{PB} \right) \Delta t / \eta_c^{TES,dis} \\ & + \left(SF_{c,k,s,m}^{Fore} - \hat{P}_{c,k,s,m}^{CSP,Cur} / \eta_c^{PB} + \hat{P}_{c,k,s,m}^{EH} / \eta_{EH} \right) \\ & \times \eta_c^{TES,cha} \Delta t, \forall k > 1, \forall c, \forall s, \forall m \end{aligned} \quad (65)$$

$$\begin{aligned} \hat{E}_{c,k,s,m}^{TES} & = \hat{E}_{c,t=N_T,s}^{TES} - \left(\hat{P}_{c,k,s,m}^{CSP} / \eta_c^{PB} \right) \Delta t / \eta_c^{TES,dis} \\ & + \left(SF_{c,k,s,m}^{Fore} - \hat{P}_{c,k,s,m}^{CSP,Cur} / \eta_c^{PB} + \hat{P}_{c,k,s,m}^{EH} / \eta_{EH} \right) \\ & \times \eta_c^{TES,cha} \Delta t, \forall k = 1, \forall c, \forall s, \forall m \end{aligned} \quad (66)$$

$$\hat{E}_c^{TES} \leq \hat{E}_{c,k,s,m}^{TES} \leq \bar{E}_c^{TES}, \forall k, \forall c, \forall s, \forall m \quad (67)$$

$$\hat{E}_{c,k,s,m}^{TES} = E_c^{TES,Ini}, \forall k = N_K, \forall c, \forall s, \forall m \quad (68)$$

Constraints (69)–(73) formulate a simplified operational model for ESS. Specifically, constraint (69) limits the charging/discharging rate of ESS. Constraints (70) formulates the energy balance in ESS. Constraint (71) links the SOC of ESS in the second-stage with that in the third stage. The SOC of ESS is limited within $[0, H_b^B P_b^{B,Max}]$ via constraint (72). Constraint (73) ensures that the SOC of ESS will go back to its initial value $E_b^{B,Ini}$ at the end of the simulating time horizon.

$$0 \leq \hat{P}_{b,k,s,m}^{B,dis}, \hat{P}_{b,k,s,m}^{B,cha} \leq P_b^{B,Max}, \forall k, \forall b, \forall s, \forall m \quad (69)$$

$$\begin{aligned} \hat{E}_{b,k,s,m}^B - \hat{E}_{b,k-1,s,m}^B & = \left(\hat{P}_{b,k,s,m}^{B,cha} / \eta_b^{B,cha} - \hat{P}_{b,k,s,m}^{B,dis} \eta_b^{B,dis} \right) \\ & \times \Delta t, \forall k > 1, \forall b, \forall s, \forall m \end{aligned} \quad (70)$$

$$\begin{aligned} \hat{E}_{b,k,s,m}^B - \tilde{E}_{b,t=N_T,s}^B & = \left(\hat{P}_{b,k,s,m}^{B,cha} / \eta_b^{B,cha} - \hat{P}_{b,k,s,m}^{B,dis} \eta_b^{B,dis} \right) \\ & \times \Delta t, \forall k = 1, \forall b, \forall s, \forall m \end{aligned} \quad (71)$$

$$0 \leq \hat{E}_{b,k,s,m}^B \leq H_b^B P_b^{B,Max}, \forall k, \forall b, \forall s, \forall m \quad (72)$$

$$\hat{E}_{b,k,s,m}^B = E_b^{B,Ini}, \forall k = N_K, \forall b, \forall s, \forall m \quad (73)$$

Overall, constraints (16) to (73) compose the proposed look-ahead three-stage stochastic operation model, which is a stochastic mixed integer linear programming (MILP) model.

C. Model Discussion

The proposed model is compactly formulated by the simplified look-ahead stochastic optimization (74), where (\mathbf{u}, \mathbf{p}) denotes the optimized UC decisions for the next-day operation scheduling. The first stage is a MILP UC model, and both the second stage and the third stage are based on LP ED model.

Since the accurate look-ahead operation for future days should employ the MILP UC model, the proposed SUC approach is a simplified one. The full look-ahead SUC model is formulated by the optimization (75), in which the look-ahead UC operation constraints are formulated as the modified version of equations (17)–(39) with neglecting the reserve schedule. This model is formulated as a MILP problem which contains much more binary variables than the simplified one and thus is time-consuming. Without considering the look-ahead operation of future days, the look-ahead SUC model is degraded to be a normal two-stage SUC optimization (76). The storage level of TES systems and storage devices reverts to the initial value at the end of next operating day.

(Simplified_LA_SUC)

$$\begin{aligned} & \text{minimize}_{\mathbf{u} \in \mathbf{U}, \mathbf{p} \in \mathbf{P}} C_{Simp}^{Three}(\mathbf{u}, \mathbf{p}) = Cost^{DA} + Cost^{RT} + Cost^{LA} \\ & \text{subject to : Day-ahead UC scheduling constraints (17)–(39)} \\ & \quad \text{Real-time ED operation constraints (40)–(55)} \\ & \quad \text{Look-ahead ED operation constraints (56)–(73)} \end{aligned} \quad (74)$$

(Full_LA_SUC)

$$\begin{aligned} & \text{minimize}_{\mathbf{u} \in \mathbf{U}, \mathbf{p} \in \mathbf{P}} C_{Full}^{Three}(\mathbf{u}, \mathbf{p}) = Cost^{DA} + Cost^{RT} + Cost^{LA} \\ & \text{subject to : Day-ahead UC scheduling constraints (17)–(39)} \\ & \quad \text{Real-time ED operation constraints (40)–(55)} \\ & \quad \text{Look-ahead UC operation constraints} \end{aligned} \quad (75)$$

(Two_Stage_SUC)

$$\begin{aligned} & \text{minimize}_{\mathbf{u} \in \mathbf{U}, \mathbf{p} \in \mathbf{P}} C_{Full}^{Two}(\mathbf{u}, \mathbf{p}) = Cost^{DA} + Cost^{RT} \\ & \text{subject to : Day-ahead UC scheduling constraints (17)–(39)} \\ & \quad \text{Real-time ED operation constraints (40)–(55)} \\ & \quad \tilde{E}_{c,t=T,s}^{TES} = E_c^{TES,Ini}, \forall c, \forall t; \tilde{E}_{b,t=T,s}^B = E_b^{B,Ini}, \forall b, \forall t \end{aligned} \quad (76)$$

The benefit of considering the look-ahead operation of future days can be evaluated as the cost difference of UC solution between the full look-ahead SUC model and the two-stage SUC model, shown in (77). The true cost performance of a UC solution can be estimated as the cost tested on the full look-ahead SUC model. Similarly, shown in (78), the cost of employing the simplified model in future days is estimated as the cost difference of UC solution between the full look-ahead SUC model and the simplified look-ahead SUC model.

Value of Look-ahead Operation:

$$C_{Full}^{Three} \left(\argmin C_{Full}^{Three}(\mathbf{u}, \mathbf{p}) \right) - C_{Full}^{Three} \left(\argmin C_{Full}^{Two}(\mathbf{u}, \mathbf{p}) \right) \quad (77)$$

Cost of Simplification:

$$C_{Full}^{Three} \left(\argmin C_{Full}^{Three}(\mathbf{u}, \mathbf{p}) \right) - C_{Full}^{Three} \left(\argmin C_{Simp}^{Three}(\mathbf{u}, \mathbf{p}) \right) \quad (78)$$

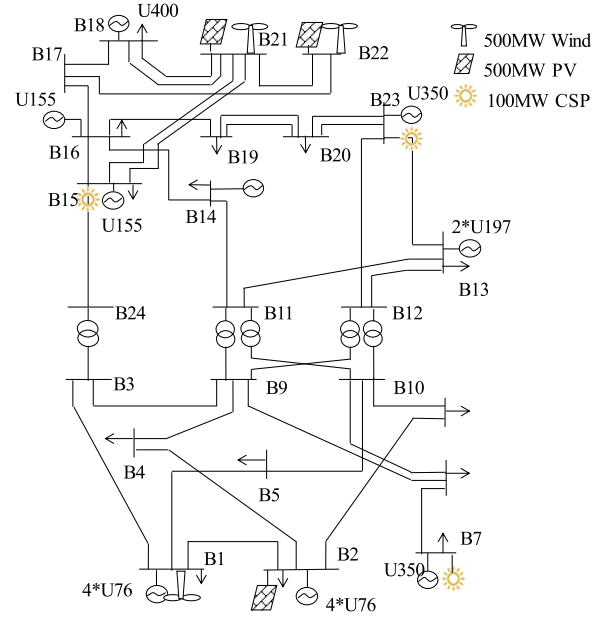


Fig. 4. Modified IEEE 24-node system.

TABLE I
GENERATOR MIX OF THE MODIFIED IEEE RTS-96 SYSTEM

	Max Load	CG	CSP	Wind	PV
Capacity/ MW	2850	2412	300	1500	1500

TABLE II
PARAMETERS OF CSP UNIT

Parameter	Value	Parameter	Value
$\Delta P^{Ru}, \Delta P^{Rd}$	40% P^{Max}	Initial SOC	50% \bar{E}^{TES}
$T_{min}^{On} (T_{min}^{Off})$	2(2) hours	$E^{PB,SU}$	50 MW-t
Solar multiple	2.4	η^{PB}	38%
TES capacity	8 hours	$\eta^{dis} (\eta^{cha})$	98% (98%)

IV. CASE STUDY

A. Test System

The proposed approach has been tested on a modified IEEE RTS-79 system which contains 24 nodes, 34 lines, and 24 generators, shown in Fig. 4. Day-ahead UC decision making is processed with considering a three-day look-ahead operation. The generation mix is given in Table I. Conventional generator data and transmission network data are extracted from [35]. Technical parameters of CSP units are listed in Table II. The SF capacity in CSP plants is measured by solar multiple (SM), which is the ratio of SF capacity to the thermal power required to operate the PB at rated capacity. The TES capacity is measured by the hours of operating the PB at rated capacity. The wind and solar data are from NREL database [34]. The load and renewable forecasting results are shown in Fig. 5. 10 real-time scenarios in the second stage and 10 look-ahead scenarios in the third stage are considered. Computations are performed us-

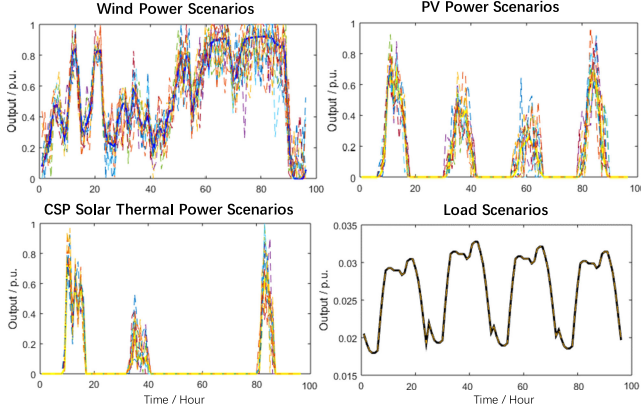


Fig. 5. Load and renewable forecasting results.

TABLE III
PERFORMANCE COMPARISON AMONG THREE MODELS

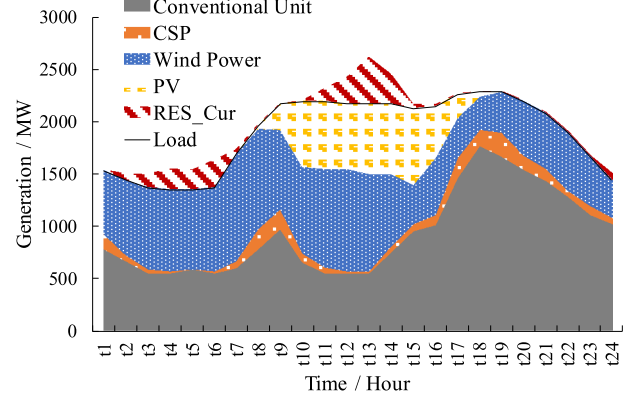
		Simplified look-ahead SUC	Full Look-ahead SUC	Two-stage SUC
Estimated Performance	Expected Operating Cost in Day1 (k\$)	216.05	221.12	222.42
	Expected Cost in Day2-Day4 (k\$)	739.20	801.26	0
	Overall Cost	955.25	1022.4	222.42
True Performance	Expected Operating Cost in Day1 (k\$)	216.05	221.12	222.42
	Expected Cost in Day2-Day4 (k\$)	860.56	801.26	882.98
	Overall Cost	1076.6	1022.4	1105.4
Benefits of Look-ahead (k\$)		28.8	83.0	-
Cost of Simplification (k\$)		54.2	-	-
Solving Time (s)		136.2	32844	80.1

ing the solver of CPLEX 12.5 on a PC with a 2.90 GHz Intel processor and 128 GB RAM.

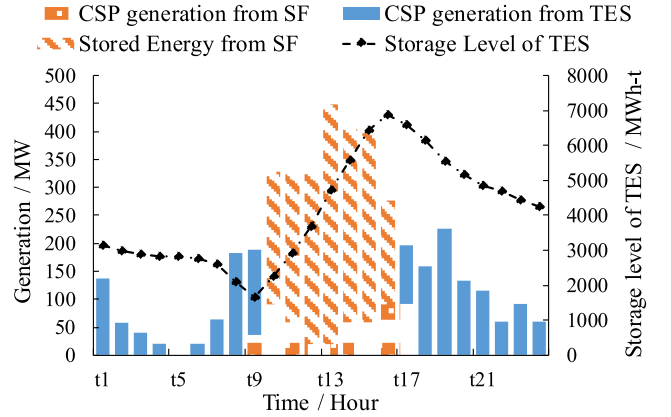
B. Verifying the Proposed Model

Three models, respectively represented by formulations (74) to (76), are tested on the above test system. Results are summarized in Table III. The estimated performance is the results coming out of the model itself. The true cost performance is the results of testing the solution on the full look-ahead SUC model. Obviously, full look-ahead SUC model involves the minimum overall cost and drives the best UC solution. However, the solving time is too long to be acceptable. The conventional two-stage SUC model has much better computational performance, but involves the worst solution, since the look-ahead future operation is not considered. The economic loss of not considering future operation is quantified as \$83.0 k. Compared with these two models, our proposed simplified look-ahead SUC model incorporates an optimistic estimation of look-ahead future operation. The solving time dramatically drops to the level similar with the two-stage SUC model.

According to the formulations (77) and (78), the saved benefit of considering future operation is \$28.8 k, and the cost of the simplification of employing look-ahead ED operation for future days in the third-stage is \$54.2 k.



(a) generation schedule



(b) operation schedule of CSP plants

Fig. 6. Day-ahead generation schedules optimized by proposed method.

According to the results from proposed SUC method, Fig. 6(a) shows how generation units are scheduled to supply demand on day-ahead stage. The renewable energy penetration level reaches up to 51.1%. The production of CSP is limited by the available solar irradiation, but is flexible in compensating for the variability of wind power and PV generation. Fig. 6(b) depicts the operating schedule of CSP plants. The absorbed solar thermal energy during the daytime is stored in the TES, instead of generating electricity. The TES system allows CSP to shift generation to the periods of sunrise and sunset.

The storage curves of TES in each scenario for different methods are compared in Fig. 7. Obviously, for the two-stage SUC method, the storage level of TES in every scenario goes back to the initial level at the end of next operating day. For two look-ahead SUC models, the residual SOC of TES at the end of next operating day is pertained to each scenario and optimized through considering the look-ahead future operation. Compared with two-stage SUC method, this brings a multi-day operation coordination.

C. Evaluating the Benefits of CSP Plants

In this section, a whole year of simulation is made to quantify the benefit of incorporating look-ahead operation in the SUC

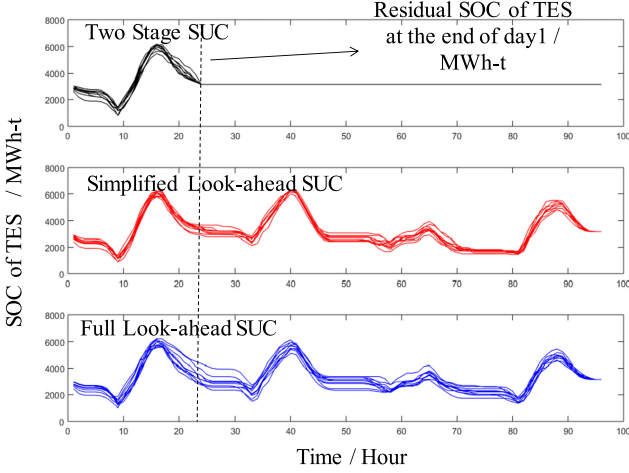


Fig. 7. Storage level of TES in each scenarios.

TABLE IV
PERFORMANCE COMPARISON AMONG CASE 1 TO CASE 6

	Overall Operating Cost (M\$)	Difference (M\$)	Renewable Curtailment (TWh)	Difference (TWh)
Case 1 (Base case)	65.72	0.0	1.08(11.7%)	0.0
Case 2 (no LA)	66.63	0.91	1.11(12.0%)	0.028
Case 3 (no CSP)	92.75	27.04	0.79(10.2%)	-0.282
Case 4 (PV)	88.06	22.34	1.85(19.9%)	0.772
Case 5 (with EH)	65.25	-0.47	0.86(9.24%)	-0.216
Case 6 (Storage)	74.37	8.65	0.36(4.69%)	-0.711

model and to preliminarily analyze the cost-effectiveness of CSP plants.

Case 1 (Base case): CSP plants are equipped with TES. The proposed look-ahead UC model is performed to strategically operate CSP to obtain a minimum-cost generation schedule.

Case 2 (no LA): Conventional two-stage SUC model is used. Thus, the look-ahead (LA) future operation is not considered.

Case 3 (no CSP): Compared with case 1, CSP plants are removed.

Case 4 (PV): Compared with case 1, 300 MW CSP plants are replaced by 710 MW PV, keeping the same annual available electricity generation.

Case 5 (with EH): Compared with case 1, CSP plants are equipped with EH to enhance the operational flexibility and make use of curtailed renewable energy generation. The transfer efficiency η_{HE} of EH is assumed to be 90%.

Case 6 (Storage): Compared with case 1, CSP plants are replaced by ESS with the same capacity. The cycle efficiency of ESS is assumed to be 75%, a typical cycle efficiency of large pumped hydro station.

The operating cost and renewable energy curtailment during a whole year in each case are compared in Table IV. Several findings are summarized. 1) Comparing case 1 with case 2, considering look-ahead future operation brings \$0.91 M saving on operating cost and reduces renewable energy curtailment by 0.028 TWh. 2) Comparing case 1 with case 3, the introduction of CSP plants brings \$27.04 M savings on operating

TABLE V
PERFORMANCE COMPARISON WITH DIFFERENT TES CAPACITY

	TES Capacity	0 Hour	4 Hour	8 Hour	12Hour
Operating Cost (M\$)	Case 1 (Base case)	88.06	69.24	65.72	64.50
	Case 2 (no LA)	88.06	70.18	66.93	65.95
	Case 5 (with EH)	88.06	69.03	65.25	63.84
Renewable Curtailment	Case 1 (Base case)	19.89%	14.56%	11.68%	10.70%
	Case 2 (no LA)	19.89%	14.69%	11.99%	11.10%
	Case 5 (with EH)	19.89%	12.90%	9.24%	7.56%

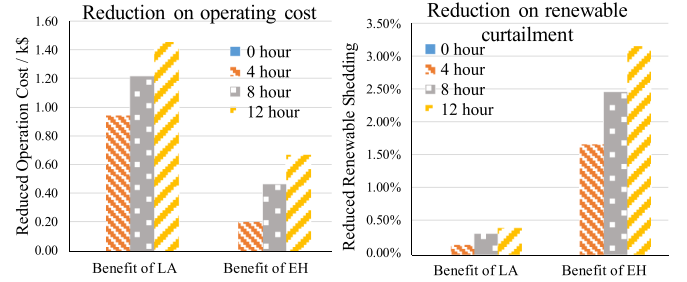


Fig. 8. Benefit of considering LA operation and benefit of equipping EH with different TES capacities.

cost, but increases renewable energy curtailment by 0.282 TWh. It should be noted that the renewable energy penetration level also increases. 3) In order to quantify the benefits of CSP's flexibility, we compare case 1 with case 4. Results show that the flexibility of CSP brings \$22.34 M savings and 0.772 TWh reduction on renewable energy curtailment. 4) Comparing case 1 with case 5, instead of curtailing surplus VRE generation, the equipment of EH allows for CSP to convert surplus VRE into thermal energy to be re-used in the future. This brings \$0.47 M operating cost savings and decreases renewable energy curtailment by 0.216 TWh. 5) Compared with the same capacity storage device, CSP is superior in reducing operating costs by \$8.65 M, but is inferior in reducing renewable energy curtailment, shedding 0.71 GWh more.

Currently, the investment cost of CSP plants with TES is very expensive. The annualized investment cost for CSP with 2.4 SM and 8-hour TES is around 700\$/kW-yr, while PV is 280\$/kW-yr [8]. Comparing case 1 and case 4 (300 MW CSP is replaced by 710 MW PV with keeping the same renewable energy penetration level), the total investment cost of CSP in case 1 is higher than the investment cost of PV in case 3 by \$11.20 M-yr, while the save annual operating cost is \$22.34 M. From this regard, investing CSP is cost-efficient. Detailed analysis method for evaluating the investment economy of CSP is left for the future study.

D. Sensitivity Analysis

1) Impact of the CSP Flexibility: The operating flexibility of CSP varies with the capacity of the TES system. Table V shows the results of cases with different TES capacity. With the increase in TES capacity, the operational flexibility of CSP is enhanced, and both the overall operating cost and the ratio of renewable energy curtailment decrease. Fig. 8 demonstrates that

TABLE VI
PERFORMANCE COMPARISON WITH DIFFERENT VRE CAPACITY

	VRE Capacity	20% Decrease	Base	20% Increase
Operating Cost (M\$)	Case 1 (Base case)	75.63	65.72	59.22
	Case 2 (no LA)	76.37	66.63	60.47
	Case 5 (with EH)	75.22	65.25	58.68
Renewable Curtailment	Case 1 (Base case)	5.86%	11.68%	18.67%
	Case 2 (no LA)	6.12%	11.99%	19.22%
	Case 5 (with EH)	4.69%	9.24%	15.75%

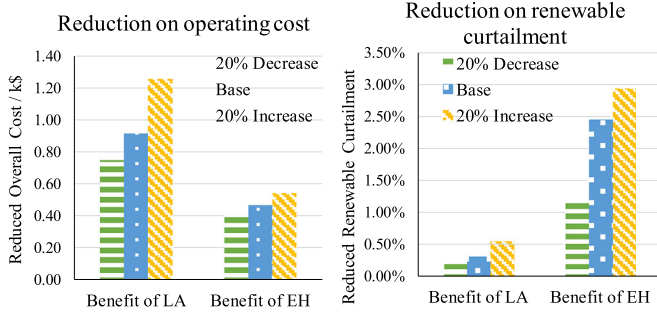


Fig. 9. Benefit of considering LA operation and benefit of equipping EH with different VRE capacities.

the benefit of considering look-ahead operation and the benefit of incorporating EH are both increased with the increase of TES capacity.

2) *Impact of the VRE Penetration:* With constant CSP capacity, we compare its performance under different renewable energy penetration levels. Table VI shows the results of the cases with the capacity of VRE increased or decreased by 20%. Obviously, with increasing VRE capacity, overall operating cost decreases, but the ratio of renewable curtailment increases. Fig. 9 demonstrates that the benefit of considering look-ahead operation and the benefit of incorporating EH are both increased with the increase of VRE capacity.

V. CONCLUSION

We address the short-term operation scheduling problem of a high renewable energy penetrated power system with the presence of CSP. A look-ahead stochastic programming model is proposed that formulates the day-ahead schedule in the first stage, real-time dispatch with uncertainty revealed in the second stage, and look-ahead operation in the third stage.

Several findings are summarized as follows:

- 1) With the presence of large scale VRE integration, CSP plants with TES are dispatch-able and have significant impact on reducing the system operating cost and the renewable energy curtailment. Specifically, CSP plants can operate strategically to shift their generation for addressing the variability of VRE generation and to provide reserves for compensating the forecast error of VRE generation.
- 2) Incorporating look-ahead future operation in day-ahead UC problems can make full use of CSP's flexibility and

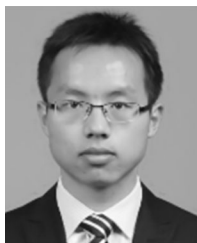
bring considerable economic benefits in reducing operating cost and renewable energy curtailment.

- 3) EH allows for CSP to convert surplus renewable energy generation into thermal energy to be re-used in future periods. Equipping CSP with EH enhances the flexibility and the economy of CSP in high renewable penetrated power systems.

REFERENCES

- [1] B. Kroposki, B. Johnson, Y. Zhang, V. Gevorgian, P. Denholm, B. M. Hodge, and B. Hannegan, "Achieving a 100% renewable grid: Operating electric power systems with extremely high levels of variable renewable energy," *IEEE Power Energy Mag.*, vol. 15, no. 2, pp. 61–73, Apr. 2017.
- [2] Y. Wang, N. Zhang, C. Kang, M. Miao, R. Shi, and Q. Xia, "An efficient approach to power system uncertainty analysis with high-dimensional dependencies," *IEEE Trans. Power Syst.*, vol. 33, no. 3, pp. 2984–2994, May 2018.
- [3] P. Denholm, Y. Wan, M. Hummon, and M. Mehos, "The value of CSP with thermal energy storage in the Western United States," *Energy Procedia*, vol. 49, pp. 1622–1631, 2014.
- [4] B. Kroposki, "Integrating high levels of variable renewable energy into electric power systems," *J. Mod. Power Syst. Clean Energy*, vol. 5, no. 6, pp. 831–837, 2017.
- [5] A. J. Conejo, Y. Cheng, N. Zhang, and C. Kang, "Long-term coordination of transmission and storage to integrate wind power," *CSEE J. Power Energy Syst.*, vol. 3, no. 1, pp. 36–43, 2017.
- [6] H. Li, A. T. Eseye, J. Zhang, and D. Zheng, "Optimal energy management for industrial micro-grids with high-penetration renewables," *Protection Control Mod. Power Syst.*, vol. 2, no. 1, pp. 1–12, 2017.
- [7] Y. Ding, C. Shao, J. Yan, Y. Song, C. Zhang, and C. Guo, "Economic flexibility options for integrating fluctuating wind energy in power systems: The case of China," *Appl. Energy*, vol. 228, pp. 426–436, 2018.
- [8] M. Hand, T. Mai, and S. Baldwin, "Renewable electricity futures study," Nat. Renewable Energy Lab., Golden, CO, USA, Tech. Rep. NREL/TP-6A20-52409, 2012.
- [9] P. Denholm and M. Mehos, "Enabling greater penetration of solar power via the use of CSP with thermal energy storage," Nat. Renewable Energy Lab., Golden, CO, USA, Tech. Rep. NREL/TP-6A20-52978, 2013.
- [10] R. Domínguez, A. J. Conejo, and M. Carrión, "Toward fully renewable electric energy systems," *IEEE Trans. Power Syst.*, vol. 30, no. 1, pp. 316–326, Jan. 2015.
- [11] R. Sioshansi and P. Denholm, "The value of concentrating solar power and thermal energy storage," *IEEE Trans. Sustain. Energy*, vol. 1, no. 3, pp. 173–183, Oct. 2010.
- [12] B. Brand, A. B. Stambouli, and D. Zejli, "The value of dispatchability of CSP plants in the electricity systems of Morocco and Algeria," *Energy Policy*, vol. 47, no. 10, pp. 321–331, 2012.
- [13] E. Du, N. Zhang, B. M. Hodge, Q. Wang, C. Kang, B. Kroposki, and Q. Xia, "The Role of Concentrating Solar Power Towards High Renewable Energy Penetrated Power Systems," *IEEE Trans. Power Syst.*, vol. 33, no. 6, pp. 6630–6641, Nov. 2018.
- [14] M. J. Vasallo and J. M. Bravo, "A MPC approach for optimal generation scheduling in CSP plants," *Appl. Energy*, vol. 165, pp. 357–370, 2016.
- [15] J. Usaola, "Operation of concentrating solar power plants with storage in spot electricity markets," *IET Renewable Power Gener.*, vol. 6, no. 1, pp. 59–66, 2012.
- [16] R. Sioshansi and P. Denholm, "Benefits of colocating concentrating solar power and wind," *IEEE Trans. Sustain. Energy*, vol. 4, no. 4, pp. 877–885, Oct. 2013.
- [17] F. J. Santos-Alamillos, D. Pozo-Vazquez, J. A. Ruiz-Arias, L. V. Bremen, and J. Tovar-Pescador, "Combining wind farms with concentrating solar plants to provide stable renewable power," *Renewable Energy*, vol. 76, pp. 539–550, 2015.
- [18] R. Chen, H. Sun, Z. Li, and Y. Liu, "Grid dispatch model and interconnection benefit analysis of concentrating solar power plants with thermal storage," (in Chinese), *Automat. Elect. Power Syst.*, vol. 38, no. 19, pp. 1–7, 2014.
- [19] H. Jin, H. Sun, Q. Guo, R. Chen, and Z. Li, "Power system multi-day stochastic scheduling considering the uncertainty of CSP/wind plants," in *Proc. IEEE Power Energy Soc. Gen. Meeting*, Boston, MA, USA, pp. 1–5, 2016.

- [20] T. Xu and N. Zhang, "Coordinated operation of concentrated solar power and wind resources for the provision of energy and reserve services," *IEEE Trans. Power Syst.*, vol. 32, no. 2, pp. 1260–1271, Mar. 2017.
- [21] P. Denholm, Y. Wan, M. Hummon, and M. Mehos, "Analysis of concentrating solar power with thermal energy storage in a California 33% renewable scenario," Nat. Renewable Energy Lab., Golden, CO, USA, Tech. Rep. NREL/TP-6A20-58186, 2013.
- [22] R. Dominguez, A. J. Conejo, and M. Carrion, "Operation of a fully renewable electricity energy system with CSP plants," *Appl. Energy*, vol. 119, pp. 417–430, 2014.
- [23] Q. P. Zheng, J. Wang, and A. L. Liu, "Stochastic optimization for unit commitment—A review," *IEEE Trans. Power Syst.*, vol. 30, no. 4, pp. 1913–1924, Jul. 2015.
- [24] J. M. Morales, A. J. Conejo, and J. Perez-Ruiz, "Economic valuation of reserves in power systems with high penetration of wind power," *IEEE Trans. Power Syst.*, vol. 24, no. 2, pp. 900–910, May 2009.
- [25] E. A. Bakirtzis, P. N. Biskas, D. P. Labridis, and A. G. Bakirtzis, "Multiple time resolution unit commitment for short-term operations scheduling under high renewable penetration," *IEEE Trans. Power Syst.*, vol. 29, no. 1, pp. 149–159, Jan. 2014.
- [26] P. Denholm and M. Hand, "Grid flexibility and storage required to achieve very high penetration of variable renewable electricity," *Energy Policy*, vol. 39, no. 3, pp. 1817–1830, 2011.
- [27] D. Pozo, J. Contreras, and E. E. Sauma, "Unit commitment with ideal and generic energy storage units," *IEEE Trans. Power Syst.*, vol. 29, no. 6, pp. 2974–2984, Nov. 2014.
- [28] N. Li, C. Uçkun, E. M. Constantinescu, J. R. Birge, K. W. Hedman, and A. Botterud, "Flexible operation of batteries in power system scheduling with renewable energy," *IEEE Trans. Sustain. Energy*, vol. 7, no. 2, pp. 685–696, Apr. 2016.
- [29] B. Lu and M. Shahidehpour, "Short-term scheduling of battery in a grid-connected PV/battery system," *IEEE Trans. Power Syst.*, vol. 20, no. 20, pp. 1053–1061, May 2005.
- [30] A. Bhattacharya, J. Kharoufeh, and B. Zeng, "Managing energy storage in microgrids: A multistage stochastic programming approach," *IEEE Trans. Smart Grid*, vol. 9, no. 1, pp. 483–496, Jan. 2018.
- [31] T. Ding, Y. Hu, and Z. Bie, "Multi-stage stochastic programming with nonanticipativity constraints for expansion of combined power and natural gas systems," *IEEE Trans. Power Syst.*, vol. 33, no. 1, pp. 317–328, Jan. 2018.
- [32] M. J. Wagner and P. Gilman, "Technical manual for the SAM physical trough model," Nat. Renewable Energy Lab., Golden, CO, USA, Tech. Rep. NREL/TP-5500-51825, 2011.
- [33] M. Mehrtash *et al.*, "Fast stochastic security-constrained unit commitment using point estimation method," *Int. Trans. Elect. Energy Syst.*, vol. 26, no. 3, pp. 671–688, 2016.
- [34] System Advisor Model, National Renewable Energy Laboratory, Golden, CO, USA, [EB/OL]. 2010. [Online]. Available: <https://sam.nrel.gov/>
- [35] Probability Methods Subcommittee, "IEEE reliability test system," *IEEE Trans. Power App. Syst.*, vol. PAS-98, no. 6, pp. 2047–2054, Nov. 1979.



Ershun Du (S'13) received the B.S. and Ph.D. degrees from the Electrical Engineering Department, Tsinghua University, Beijing, China, in 2013 and 2018, respectively. His research interests include renewable energy uncertainty analysis, power system operation and planning with wind power, photovoltaic, and concentrating solar power.



Ning Zhang (M'12–SM'18) received the B.S. and Ph.D. degrees from the Electrical Engineering Department, Tsinghua University, Beijing, China, in 2007 and 2012, respectively. He is currently an Associate Professor with Tsinghua University. His research interests include multiple energy system integration power system planning and scheduling with renewable energy, and stochastic analysis and simulation of renewable energy.



Bri-Mathias Hodge (M'09–SM'17) received the B.S. degree in chemical engineering from Carnegie Mellon University, Pittsburgh, PA, USA, in 2004, the M.S. degree from the Process Design and Systems Engineering Laboratory, Åbo Akademi University, Turku, Finland, in 2005, and the Ph.D. degree in chemical engineering from Purdue University, West Lafayette, IN, USA, in 2010. He is currently the Manager with the Power System Design and Studies Group, National Renewable Energy Laboratory, Golden, CO, USA.



Qin Wang (M'13) received the Ph.D. degree from the Electrical and Computer Engineering Department, Iowa State University, Ames, IA, in 2013. He is currently a Senior Engineer/Scientist with the Electric Power Research Institute, Palo Alto, CA, USA. His previous industry experiences include positions with National Renewable Energy Laboratory, Midcontinent ISO, and ISO New England. His research interests include power system reliability and online security analysis, smart distribution systems, trans-active energy, transmission planning, and electricity markets.



Zongxiang Lu (M'02) received the B.S. and Ph.D. degrees from the Electrical Engineering Department, Tsinghua University, Beijing, China, in 1998 and 2002, respectively. He is currently an Associate Professor with Tsinghua University. His research interests include large-scale wind/PV integration analysis and control, energy and electricity strategy planning, power system reliability, DG, and microgrid.



Chongqing Kang (M'01–SM'07–F'17) received the Ph.D. degree from the Electrical Engineering Department, Tsinghua University, Beijing, China, in 1997. He is currently a Professor with Tsinghua University. His research interests include low-carbon electricity, power system planning, renewable energy, power markets, and power system load forecasting.



Benjamin Kroposki (M'92–SM'00–F'14) received the B.S. and M.S. degrees in electrical engineering from Virginia Tech, Blacksburg, VA, USA, and the Ph.D. degree from Colorado School of Mines, Golden, CO, USA. He is currently the Director of the Power Systems Engineering Center, National Renewable Energy Laboratory, Golden, CO, USA. His research interests include design, testing, and integration of renewable and distributed power systems.



Qing Xia (M'01–SM'08) received the Ph.D. degree from the Electrical Engineering Department, Tsinghua University, Beijing, China, in 1989. He is currently a Professor with Tsinghua University. His research interests include electricity markets, generation schedule optimization, and power system planning.